applied sciences

MDPI

Communication

$Pyr_{1,x}TFSI$ Ionic Liquids (x = 1–8): A Computational Chemistry Study

Sergio Brutti [1,2,3]

[1] Department of Chemistry, University of Rome La Sapienza, Piazzale Aldo Moro 5, 00185 Rome, Italy; sergio.brutti@uniroma1.it
[2] CNR-ISC, U.O.S. La Sapienza, Piazzale A. Moro 5, 00185 Rome, Italy
[3] GISEL—Centro di Riferimento Nazionale per i Sistemi di Accumulo Elettrochimico di Energia, INSTM via G. Giusti 9, 50121 Firenze, Italy

Received: 1 October 2020; Accepted: 26 November 2020; Published: 29 November 2020

Featured Application: Novel electrolyte solvents for aprotic secondary batteries based on Li, Na or other alkaline/alkaline metal elements.

Abstract: Pyrrolidinium-based (Pyr) ionic liquids are a very wide family of molecular species. Pyrrolidinium cations are electrochemically stable in a large potential interval and their molecular size hinders their transport properties. The corresponding ionic liquids with trifluoromethyl sulphonyl imide anions are excellent solvents for lithium/sodium salts and have been demonstrated as electrolytes in aprotic batteries with enhanced safety standards. In this study, the analysis of the physicochemical properties of a homologous series of pyrrolidinium-based ionic liquids with general formula $Pyr_{1,x}TFSI$ (x = 1–8) have been tackled by first principles calculations based on the density functional theory. The molecular structures of isolated ions and ion pairs have been predicted by electronic structure calculations at B3LYP level of theory in vacuum or in simulated solvents. Thermodynamic properties have been calculated to evaluate the ion pairs dissociation and oxidation/reduction stability. This is the first systematic computational analysis of this series of molecules with a specific focus on the impact of the length of the alkyl chain on the pyrrolidinium cation on the overall physicochemical properties of the ion pairs.

Keywords: ionic liquids; density functional theory (DFT); computational chemistry

1. Introduction

Ionic liquids are a very wide class of materials with extremely varied properties and highly diversified potential ranges of application [1,2]. Their use as solvents in battery electrolytes was proposed in the early 2000s and has so far been demonstrated for an extremely large number of ionic couples (e.g., pyrrolidinium, pyridinium, ammonium, imidazolium cations couples with hexafluorophosphate, bis-trifluoromethyl sulphonyl imide, trifluoromethyl sulphonate, and any other anions) [3–5]. Methyl-alkyl pyrrolidinium-based ($Pyr_{1,x}$) bis-trifluoromethyl sulphonyl imide (TFSI) ionic liquids have found in particular successful applications in many different novel aprotic battery formulations thank to their (a) large electrochemical stability, (b) facile synthesis, (c) extended thermal stability, and (d) good transport properties [6–11]. The ability of $Pyr_{1,x}TFSI$ ionic liquids to dissolve lithium and sodium salts [6–8] in particular allows researchers to obtain concentrated electrolytes suitable for real applications in Li-ion and Na-ion batteries with superior performance in terms of thermal stability [9,10] and hazard mitigation [11]. Overall, the development of a new electrolyte formulation for any aprotic battery chemistry requires a complex compromise to balance different functional properties such as electrochemical stability, transport, viscosity, thermal stability,

chemical stability, or stability of the metal ion coordination shells [12,13]. Thus, knowledge of the physicochemical properties, such as ion pair structure, dissociation energies, and oxidation/reduction potentials, is fundamental to drive the screening and selection of innovative solvents [13].

In this study, the analysis of the physicochemical properties of a homologous series of pyrrolidinium-based ionic liquids with general formula $Pyr_{1,x}TFSI$ (x = 1–8) have been tackled by first principles calculations based on the density functional theory using the Gaussian09 suite [14–16]. The molecular structures of isolated ions and ion pairs have been predicted by electronic structure calculations at B3LYP [14,15] level of theory in vacuum or in simulated solvents. Thermodynamic properties have been calculated to evaluate the ion pairs dissociation and oxidation/reduction stability.

In the literature, the structure and physicochemical properties of $Pyr_{1,x}TFSI$ ionic liquids have been studies widely by many authors (see, as an example, Triolo and coworkers [15,16], Passerini and coworkers [4,7,17], and us [9,10]). These ionic molecules self-organize in the liquid phase in meso-domains where ionic and amphiphilic molecular fragments are clustered. This structural organization leads to the facile mobility of small size ions like Li^+ [10,17] and the easy dissociation of alkaline metal salts in a wide concentration range [6,7]. Experimentally, the electrochemical stability and transport properties of many $Pyr_{1,x}TFSI$ ionic liquids have been reported [3,7,8,10,17] but a rational analysis of the impact of the size of the methyl-pyrrolidinium alkyl chain has not been reported so far. The study presented here is the first systematic computational analysis of $Pyr_{1,x}TFSI$ (x = 1–8) molecules with a specific focus on the impact of the length of the alkyl chain on the overall physicochemical properties of the ion pair.

2. Materials and Methods

The density functional theory (DFT) was adopted to calculate molecular properties of ions and ion pairs and to make thermodynamic predictions following the same approach validated by us in [18]. A B3LYP functional [19] was adopted within the 6–31++g(d,p) basis set [20] in the final calculations. The choice of the B3LYP functional has been done to follow the same computational approach illustrated by Angenendt [21] and considering [18]. In this last study, we estimated the mean accuracy of various density functionals (either purely DFT or hybrid) compared to post-Hartree Fock (post-HF) methods. Apparently, post-HF methods, like MP2, are still too computational expensive to deal with large molecules with few tenths of atoms, thus B3LYP is still an optimal compromise to achieve reasonable accuracy on energetics. Based on our previous method validation, the computational accuracy has been evaluated in approximately 8 kJ mol^{-1}. In all calculations, we incorporated solvation effects by employing a self-consistent reaction field in continuum solvation model C-PCM [22,23]. As model solvents, we used tetrahydrofurane (dielectric constant ε = 7.42) to mimic the low dielectric constant of $Pyr_{1,x}TFSI$ pure ionic liquids [24,25].

Simulating ion pairs requires a careful screening of the multiple possible configurations. Here, four ion pairs configurations were pre-evaluated for each molecular system to identify the most stable one. The computational protocol follows this procedure: (a) cations and ions are optimized individually in vacuum and in simulated solvent using the level of theory discussed above; (b) four different starting structures for each ion pair are identified using the SECIL code [21] that generates automatically and "mindlessly" a preset number of pair configurations; (c) these preliminary configurations are relaxed to local minima using the Hartree–Fock 6–31 g(d,p) method and the simulated solvent; (d) for each ion-pair, the configuration with the minimal total energy was selected.

All molecular structures were relaxed to their minima: frequency calculations were performed to check that the minima all have real vibrational frequencies. The basis set superimposition error (BSSE) correction37 has been evaluated at the same level of theory for all ion pairs. All calculations have been carried out by using the Gaussian09 package [14]. The cartesian atomic position of all the optimized structures of ion pairs are reported in the Supplementary Material (Tables S1–S8). Molecular sizes have been calculated by evaluating the volume inside a contour of 0.001 electrons $Bohr^{-3}$ density.

Ion pair Gibbs energy of dissociation energies in ions, i.e., $\Delta_{diss}G°_{298K}$, were obtained from the total energies by the simple equation:

$$\Delta_{diss}G^{o}_{298K} = \left[G^{o}_{298K}(cation) + G^{o}_{298K}(anion)\right] - G^{o}_{298K}(ion\ pair).$$

Ionization energies (E_{ion}) of anions were obtained in vacuum from the energy of each ions and the corresponding neutral molecule (open shell, doublet spin state) with one missing electron. The Franck–Condon approximation was assumed (vertical transitions), and thus, the energies of the neutral radicals were calculated from the nonrelaxed geometry of the corresponding anions following the method described by Truhlar and coworkers [26,27]. A similar approach has been adopted for the ionization energies of ion pairs as well as for the electron affinities (EA) of cations and neutral ion pairs. EA and E_{ion} were converted to approximate oxidation and reduction potentials vs. Li^+/Li, accordingly to what was suggested by Johansson and coworkers [12,28]. In particular, to convert the EA and E_{ion}, in units of eV, to a relative potential in reference to the Li^+/Li redox couple, a constant value (k) was subtracted from the calculated absolute potential. It is known and widely accepted that the reference half reaction behind the SHE—the Standard Hydrogen Electrode— has an experimental absolute oxidation potential close to 4.5 eV [26,27]. Since the Li^+/Li couple is at −3.04 V vs. SHE, the calculated oxidation potential can be compared to the Li+/Li reference by relating it to an absolute value of 1.46 eV.

3. Results

3.1. Ion Pairs Structure

A visual summary of the molecular structures of the ion pairs analyzed is shown in Figure 1.

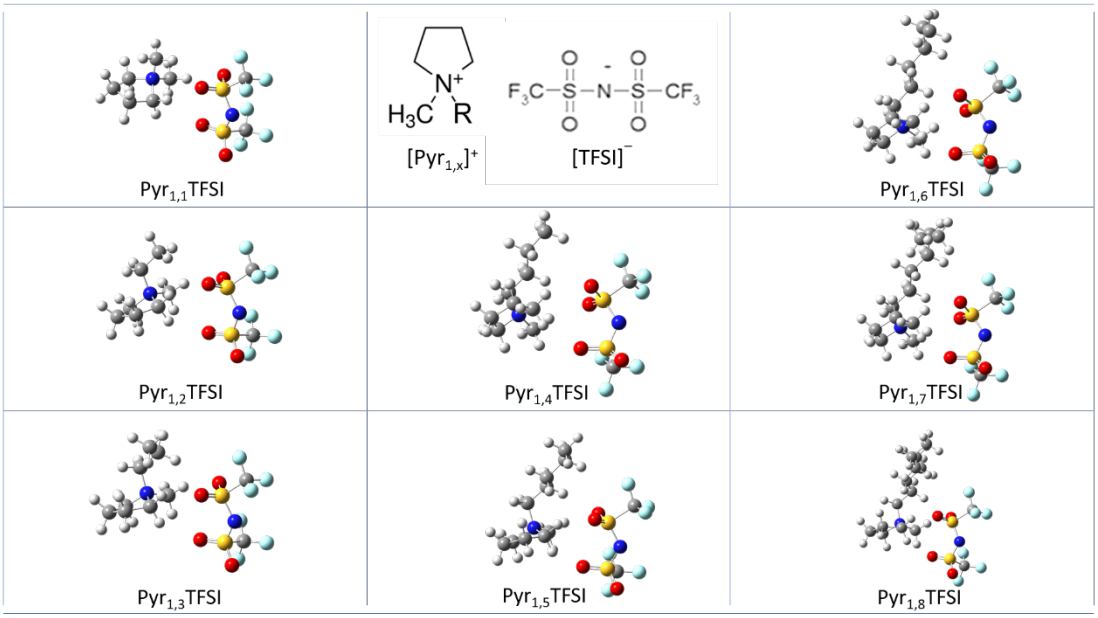

Figure 1. Molecular structures of the studied ionic couples $Pyr_{1,}$ x TFSI (x = 1–8).

In all cases, the [$Pyr_{1,x}^+$ ··$TFSI^-$] ion pairs assemble by facing the partial negative charges concentrated on the oxygen atoms of the sulphonyl groups on the $TFSI^-$ anion and the positive charges delocalized over the alkyl chains on the $Pyr_{1,x}^+$ cations. In particular, in all pyrrolidinium rings, the positive charge is distributed on the carbon atoms directly bonded to the quaternary nitrogen atom thus leading to highly delocalized cations. Nitrogen atoms are negatively charged on both ions.

As expected, the increase of the size of the lateral alkyl chain on the pyrrolidinium cation leads to an increase of the molecular volume as shown in Figure 2a. On the other hand, the distance between

the negatively charged nitrogen atoms on the TFSI2$^-$ anion and the $Pyr_{1,x}^+$ cations has a nonmonotonic trend (see Figure 2a). In particular, the nitrogen atoms increase their distance from 5.45 to 5.62 A, passing from x = 1 to x = 4, whereas the N ··N distance drops below 5.4 A for longer alkyl chains (x > 4). This trend closely matches the evolution of the partial negative charges on both nitrogen atoms (see Figure 2b). The analytical report of the charges on all atoms in all ion pairs is reported in the Supplementary Materials (Tables S1–S8).

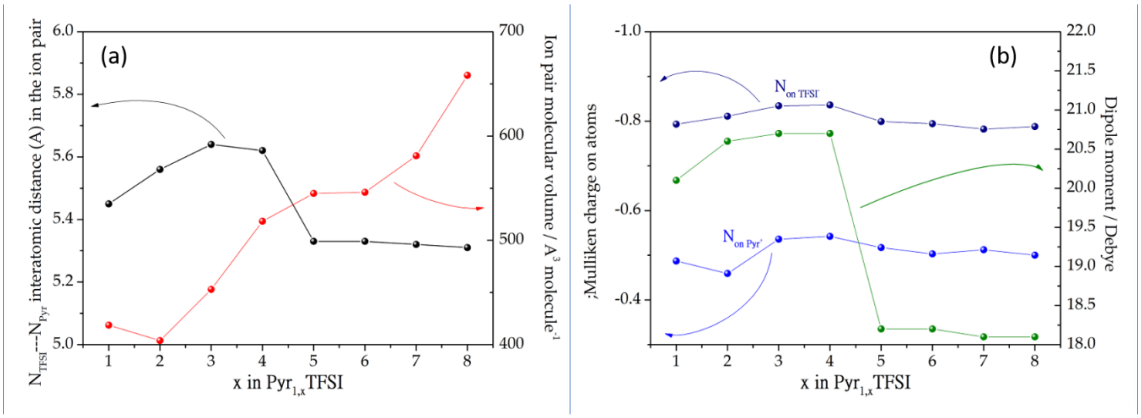

Figure 2. (**a**) Size of the ion pair and N–N interatomic distance in the ionic couple in function of the length of the pyrrolidinium later alkyl chain; (**b**) evolution of the Mulliken charges on the nitrogen atoms in the ionic couples in function of the length of the pyrrolidinium later alkyl chain in comparison with the dipole moment.

These parallel trends highlight the alteration of the structures of the ion pairs passing from short to long lateral alkyl chains on the pyrrolidinium cation. In fact, longer later alkyl chains apparently weaken the ion pair coupling in small $Pyr_{1,x}^+$ (x = 1–4) cations. This effect leads to an increase of the dipole moments. On the contrary, in large $Pyr_{1,x}^+$ (x = 5–8) cations, the decrease of the negative charges on the nitrogen atoms leads to a closer coupling of the ion pairs, thus resulting to a drastic drop in the dipole moment.

In summary, the structure of the $Pyr_{1,x}$TFSI ion pairs alters with the elongation of the lateral alkyl chain on the pyrrolidinium cation. The volume on the neutral pairs increases monotonically but ions are more distant passing from x = 1 to x = 4, whereas from x = 5 to x = 8, the ionic couple is packed more efficiently. This nonmonotonic trend is likely driven by the delocalization of the negative charge of the nitrogen atom on the pyrrolidinium cation with long alkyl chains. This structural evolution has a remarkable impact on the dipole moment of the ion pair that reaches a maximum for $Py_{1,3}$TFSI and $Pyr_{1,4}$TFSI and then has drops of approximately 10% for longer alkyl chains.

3.2. Dissociation Thermodynamics

The thermodynamics of the dissociation reactions of the ion pairs in the simulated solvent is summarized in Table 1 in comparison with the dissociation of the LiTFSI in the same conditions.

All the ionic couples are only weakly bonded, and the interionic coupling shows a trend closely matching the evolution of the structure (see previous section). In fact, the elongation of the alkyl chains on the pyrrolidinium cations from x = 1 to x = 4 weakens the ionic interaction, resulting in a slight increase of the Gibbs energy of dissociation. On the oppositive, the closer packing of the ionic couple observed form longer alkyl chains (from x = 5 to x = 8) on the pyrrolidinium cation leads to almost null dissociation energies. It is remarkable to note that the LiTFSI salt, typically used electrolytes for Li-ion batteries constituted by TSFI-based ionic liquids [9,10], has a largely positive dissociation Gibbs energy at 298 K. These thermodynamic features suggests that electrolytes constituted by $Pyr_{1,x}$TFSI solvents and LiTFSI salts are constituted by weakly interacting $Pyr_{1,x}^+$ and TFSI$^-$ ions that coordinate strongly bonded Li^+···TFSI$^-$ pairs. In this respect, the elongation of the alkyl chain on the pyrrolidinium cation

is expected to impact on the mobility of Li^+ ions due to the increase of the ionicity of the solution. This ionicity increase, induced by the larger dissociation of the ionic liquid pairs with longer alkyl chains, may enhance the viscosity of the solution at the same salt concentration but may also alter the mesoscopic structuration of the ionic/amphiphilic domains of the ionic liquid phase [15,16].

Table 1. Summary of the Gibbs energy of dissociation of the various ionic liquids.

Dissociation Reaction	Gibbs Energy of Dissociation at 298 K $\Delta_{diss}G^o_{298K}$/kJ mol^{-1}
$Pyr_{1,1}TFSI \rightarrow Pyr_{1,1}^+ + TFSI^-$	2.6
$Pyr_{1,2}TFSI \rightarrow Pyr_{1,1}^+ + TFSI^-$	4.7
$Pyr_{1,3}TFSI \rightarrow Pyr_{1,1}^+ + TFSI^-$	5.9
$Pyr_{1,4}TFSI \rightarrow Pyr_{1,1}^+ + TFSI^-$	8.7
$Pyr_{1,5}TFSI \rightarrow Pyr_{1,1}^+ + TFSI^-$	3.0
$Pyr_{1,6}TFSI \rightarrow Pyr_{1,1}^+ + TFSI^-$	1.8
$Pyr_{1,7}TFSI \rightarrow Pyr_{1,1}^+ + TFSI^-$	0.3
$Pyr_{1,8}TFSI \rightarrow Pyr_{1,1}^+ + TFSI^-$	0.4
$LiTFSI \rightarrow Li^+ + TFSI^-$	540

3.3. Electrochemical Stability

The computed reduction and oxidation potentials of the ionic pairs are shown in Figure 3.

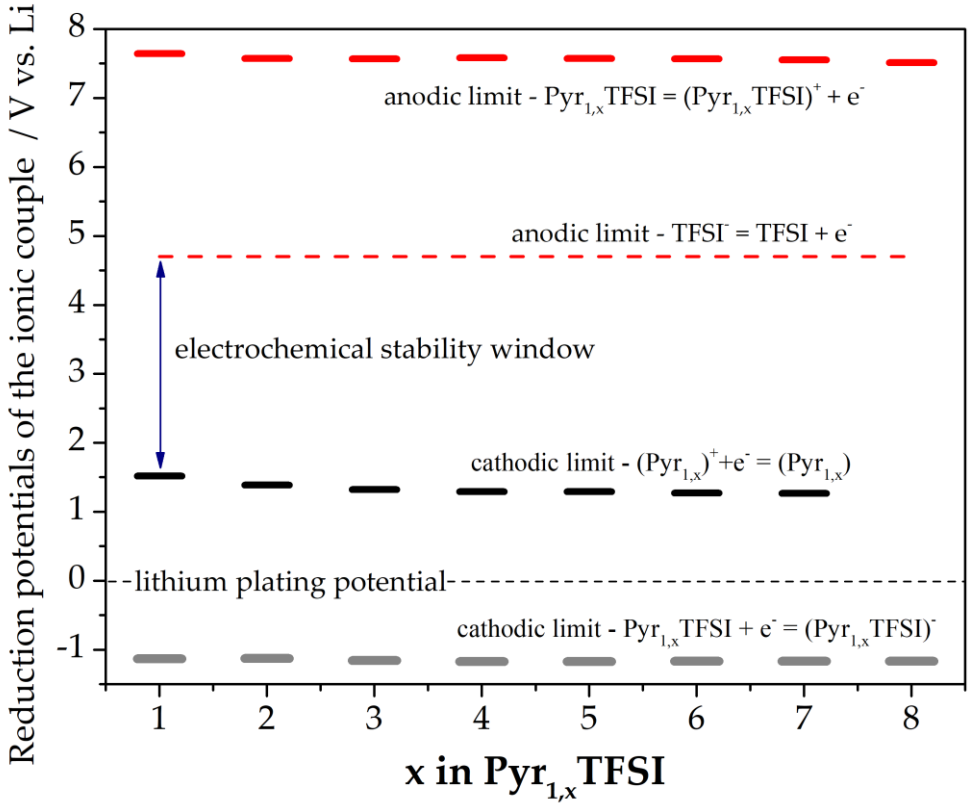

Figure 3. Predicted electrochemical stability windows for the $Pyr_{1,x}TFSI$ (x = 1–8) ionic liquids.

The electrochemical stability, both in reduction and in oxidation, of the $Pyr_{1,x}TFSI$ ionic liquids are apparently barely affected by the elongation of the later alkyl chain on the pyrrolidinium cation. Remarkably the electrochemical stability of the isolated ions is much smaller compared to ionic couples. This discrepancy likely suggests a remarkable impact on the effective oxidation and reduction onset potential of the ionic association in liquid electrolytes.

These computational estimates can be compared with the few available experimental electrochemical stability values reported in the literature by means of voltametric runs [9,10,29–35]. The cathodic stability of the $Pyr_{1,N}TFSI$ solvents (N = 3–7) ranges between 0 and −0.2 V vs. Li^+/Li: our predictions are in excellent agreement with these experimental determinations, thus confirming the reliability of the methodology. Turning to the anodic stability, for Pyr1,4TFSI, many reports observed values ranging between 4.2 to 5.5 V vs. Li^+/Li, whereas less is known for the other molecules in the series. In this view, our predictions are the first systematic report. It should be noted that the electrochemical oxidation and reduction potentials are strongly dependent on the nature of the working electrode surface/composition (e.g., Pt, Pd, stainless steel, carbon coated copper, copper, aluminum) and well as on the voltametric experimental conditions (scan rate, potential holds, temperature, nature of the counter electrode, nature of the reference electrode). In the case of reduction potentials, a further critical point is the overlap of the degradation chemistry of the ionic liquid molecules with the plating reaction of alkaline metals on the working electrode when lithium/sodium counter electrodes are used.

Overall, our analysis confirms that all $Pyr_{1,x}TFSI$ have an electrochemical stability that is suitable for application as electrolyte solvents in aprotic batteries (both Na- or Li-based). In fact, the typical positive electrodes working potentials ranges between 3.5 and 4.5 V vs. Li [36] whereas negative electrodes operate at potentials between 1.5 and few mV vs. Li (e.g., $Li_4Ti_5O_{12}$, graphite) [37,38].

4. Conclusions

In this work, the analysis of the thermodynamic and physicochemical properties of the $Pyr_{1,x}TFSI$ (x = 1–8) ion pairs have been modeled in simulated solvent in order to mimic the properties of the corresponding ionic liquids. DFT calculations have been performed to predict the structure of the ion pairs, their dissociation thermodynamics, and electrochemical stability.

In summary, this study suggests to group this family of ionic pairs in two subgroups: short-chain (X = 1–4) and long-chain (x ≥ 5) ionic liquids based on the length of the lateral alkyl chain on the methyl-pyrrolidinium cation. The volume on all ion pairs increases monotonically but cations and anions are more distant passing from x = 1 to x = 4, whereas from x = 5 to x = 8, the ionic couple is packed more efficiently. This nonmonotonic trend is likely driven by the delocalization of the negative charge of the nitrogen atom on the pyrrolidinium cation with long alkyl chains. Similarly, the elongation of the alkyl chains on the pyrrolidinium cations from x = 1 to x = 4 weakens the ionic interaction resulting from a Gibbs energy of dissociation that increases from slightly negative to slightly positive. On the oppositive, the closer packing of the ionic couple observed form longer alkyl chains (from x = 5 to x = 8) on the pyrrolidinium cation leads to slightly negative dissociation energy. On the contrary, the electrochemical stability shows similar behaviors between short-chain and long-chain ion pairs.

Overall, this study suggests that the use of $Pyr_{1,x}TFSI$ ionic liquid with longer alkyl chains compared to the typical $Pyr_{1,4}TFSI$ [9] may provide advantages due to the closer but weaker coupling of the ionic pair in the liquid phase. Further analyses are in progress to extend the description of these molecular systems while considering charged adducts (e.g., $Pyr_{1,N}(TFSI)_2^-$ or $(Pyr_{1,N})_2TFSI^+$) as well as higher levels of theory including dispersion interactions.

Supplementary Materials: The following are available online at http://www.mdpi.com/2076-3417/10/23/8552/s1, Table S1: Atomic coordinates and Mulliken charges of the $Pyr_{1,1}TFSI$ ion pair. Table S2: Atomic coordinates and Mulliken charges of the $Pyr_{1,2}TFSI$ ion pair. Table S3: Atomic coordinates and Mulliken charges of the $Pyr_{1,3}TFSI$ ion pair. Table S4: Atomic coordinates and Mulliken charges of the $Pyr_{1,4}TFSI$ ion pair. Table S5: Atomic coordinates and Mulliken charges of the $Pyr_{1,5}TFSI$ ion pair. Table S6: Atomic coordinates and Mulliken charges of the $Pyr_{1,6}TFSI$ ion pair. Table S7: Atomic coordinates and Mulliken charges of the $Pyr_{1,7}TFSI$ ion pair. Table S8: Atomic coordinates and Mulliken charges of the $Pyr_{1,8}TFSI$ ion pair.

Funding: This research was funded by the University of Rome La Sapienza through the grant number RM11916B8879F09D.

Conflicts of Interest: The author declares no conflict of interest.

References

1. Sandhu, J.S. Recent advances in ionic liquids: Green unconventional solvents of this century: Part I. *Green Chem. Lett. Rev.* **2011**, *4*, 289–310. [CrossRef]
2. Lei, Z.; Chen, B.; Koo, Y.M.; Macfarlane, D.R. Introduction: Ionic Liquids. *Chem. Rev.* **2017**, *117*, 6633–6635. [CrossRef] [PubMed]
3. Lewandowski, A.; Świderska-Mocek, A. Ionic liquids as electrolytes for Li-ion batteries—An overview of electrochemical studies. *J. Power Sources* **2009**, *194*, 601–609. [CrossRef]
4. Kalhoff, J.; Eshetu, G.G.; Bresser, D.; Passerini, S. Safer electrolytes for lithium-ion batteries: State of the art and perspectives. *ChemSusChem* **2015**, *8*, 2154–2175. [CrossRef]
5. Armand, M.; Endres, F.; MacFarlane, D.R.; Ohno, H.; Scrosati, B. Ionic-liquid materials for the electrochemical challenges of the future. *Nat. Mater.* **2009**, *8*, 621–629. [CrossRef]
6. Suo, L.; Hu, Y.S.; Li, H.; Armand, M.; Chen, L. A new class of Solvent-in-Salt electrolyte for high-energy rechargeable metallic lithium batteries. *Nat. Commun.* **2013**, *4*, 1481. [CrossRef]
7. Johansson, P.; Fast, L.E.; Matic, A.; Appetecchi, G.B.; Passerini, S. The conductivity of pyrrolidinium and sulfonylimide-based ionic liquids: A combined experimental and computational study. *J. Power Sources* **2010**, *195*, 2074–2076. [CrossRef]
8. Brutti, S.; Navarra, M.A.; Maresca, G.; Panero, S.; Manzi, J.; Simonetti, E.; Appetecchi, G.B. Ionic liquid electrolytes for room temperature sodium battery systems. *Electrochim. Acta* **2019**, *306*, 317–326. [CrossRef]
9. Lombardo, L.; Brutti, S.; Navarra, M.A.; Panero, S.; Reale, P. Mixtures of ionic liquid e Alkylcarbonates as electrolytes for safe lithium-ion batteries. *J. Power Sources* **2013**, *227*, 8–14. [CrossRef]
10. Celeste, A.; Silvestri, L.; Agostini, M.; Sadd, M.; Palumbo, S.; Panda, J.K.; Matic, A.; Pellegrini, V.; Brutti, S. Enhancement of Functional Properties of Liquid Electrolytes for Lithium-Ion Batteries by Addition of Pyrrolidinium-Based Ionic Liquids with Long Alkyl-Chains. *Batter. Supercaps* **2020**, *3*, 1051–1068. [CrossRef]
11. Arbizzani, C.; Gabrielli, G.; Mastragostino, M. Thermal stability and flammability of electrolytes for lithium-ion batteries. *J. Power Sources* **2011**, *196*, 4801–4805. [CrossRef]
12. Johansson, P.; Jacobsson, P. Rational design of electrolyte components by ab initio calculations. *J. Power Sources* **2006**, *153*, 336–344. [CrossRef]
13. Matsumoto, R.; Thompson, M.W.; Cummings, P.T. Ion Pairing Controls Physical Properties of Ionic Liquid-Solvent Mixtures. *J. Phys. Chem. B* **2019**, *123*, 9944–9955. [CrossRef] [PubMed]
14. Frisch, M.J.; Trucks, G.W.; Schlegel, H.B.; Scuseria, G.E.; Robb, M.A.; Cheeseman, J.R.; Scalmani, G.; Barone, V.; Petersson, G.A.; Nakatsuji, H.; et al. *Gaussian 16, Revision C.01*; Gaussian, Inc.: Wallingford, CT, USA, 2016.
15. Russina, O.; Triolo, A. Ionic Liquids and Neutron Scattering. In *Experimental Methods in the Physical Sciences*; Academic Press: Cambridge, MA, USA, 2017; Volume 49, pp. 213–278.
16. Russina, O.; lo Celso, F.; Plechkova, N.; Jafta, C.J.; Appetecchi, G.B.; Triolo, A. Mesoscopic organization in ionic liquids. *Top. Curr. Chem.* **2017**, *375*, 58. [CrossRef] [PubMed]
17. Castiglione, F.; Moreno, M.; Raos, G.; Famulari, A.; Mele, A.; Appetecchi, G.B.; Passerini, S. Structural organization and transport properties of novel pyrrolidinium-based ionic liquids with perfluoroalkyl sulfonylimide anions. *J. Phys. Chem. B* **2009**, *113*, 10750–10759. [CrossRef]
18. Carboni, M.; Spezia, R.; Brutti, S. Perfluoroalkyl-Fluorophosphate Anions for High Voltage Electrolytes in Lithium Cells: DFT Study. *J. Phys. Chem. C* **2014**, *118*, 24221–24230. [CrossRef]
19. Becke, A.D. Density-functional exchange-energy approximation with correct asymptotic behavior. *Phys. Rev. A* **1988**, *38*, 3098–3100. [CrossRef]
20. McLean, A.D.; Chandler, G.S. Contracted Gaussian basis sets for molecular calculations. I. Second row atoms, Z = 11–18. *J. Chem. Phys.* **1980**, *72*, 5639.
21. Angenendt, K.; Johansson, P. Ionic liquid structured from large density functional theory calculations using mindless configurations. *J. Phys. Chem. C* **2010**, *114*, 20577–20582. [CrossRef]
22. Barone, V.; Cossi, M. Quantum Calculation of Molecular Energies and Energy Gradients in Solution by a Conductor Solvent Model. *J. Phys. Chem. A* **1998**, *102*, 1995–2001. [CrossRef]
23. Cossi, M.; Rega, N.; Scalmani, G.; Barone, V. Energies, structures, and electronic properties of molecules in solution with the C-PCM solvation model. *J. Comput. Chem.* **2003**, *24*, 669–681. [CrossRef] [PubMed]
24. Weingärtner, H. The static dielectric permittivity of ionic liquids. *J. Mol. Liq.* **2014**, *192*, 185–190. [CrossRef]

25. Singh, T.; Kumar, A. Static dielectric constant of room temperature ionic liquids: Internal pressure and cohesive energy density approach. *J. Phys. Chem. B* **2008**, *112*, 12968–12972. [CrossRef] [PubMed]
26. Ho, J.; Coote, M.L.; Cramer, C.J.; Truhlar, D. Theoretical calculation of reduction potentials. In *Organic Electrochemistry: Revised and Expanded*; CRC Press: Boca Raton, FL, USA, 2015; Volume 6.
27. Winget, P.; Cramer, C.J.; Truhlar, D.G. Computation of equilibrium oxidation and reduction potentials for reversible and dissociative electron-transfer reactions in solution. *Theor. Chem. Acc.* **2004**, *112*, 217–227. [CrossRef]
28. Jónsson, E.; Johansson, P.; Xu, K. Electrochemical oxidation stability of anions for modern battery electrolytes: A CBS and DFT study. *Phys. Chem. Chem. Phys.* **2015**, *17*, 3697–3703. [CrossRef]
29. Brutti, S.; Simonetti, E.; De Francesco, M.; Sarra, A.; Paolone, A.; Palumbo, O.; Fantini, S.; Lin, R.; Falagayrat, A.; Choi, H.; et al. Ionic liquid electrolytes for high-voltage lithium batteries. *J. Sources* **2020**, *479*, 238791.
30. Bellusci, M.; Simonetti, E.; De Francesco, M.; Appetecchi, G.B. Ionic liquid electrolytes for safer and more reliable sodium battery systems. *Appl. Sci.* **2020**, *10*, 6323. [CrossRef]
31. Howlett, P.C.; MacFarlane, D.R.; Hollenkamp, A.F. High lithium metal cycling efficiency in a room-temperature ionic liquid. *Electrochem. Solid State Lett.* **2004**, *7*, A97–A101. [CrossRef]
32. Kim, G.T.; Appetecchi, G.B.; Montanarino, M.; Alessandrini, F.; Passerini, S. Long-term cyclability of lithium metal electrodes in ionic liquid-based electrolytes at room temperature. *ECS Trans.* **2010**, *25*, 12138. [CrossRef]
33. Randstrom, S.; Appetecchi, G.B.; Lagergren, C.; Moreno, A.; Passerini, S. The Influence of aur and its components on the cathodic stability of N-butyl-N-methylpyrrolidinium bis(trifluoromethanesulphonyl)imide. *Electrochim. Acta* **2007**, *53*, 1837–1842. [CrossRef]
34. Randstrom, S.; Montanino, M.; Appetecchi, G.B.; Legergren, C.; Moreno, A.; Passerini, S. Effect of water and oxygen traces on the cathodic stability of N-alkyl-N-methylpyrrolidinium bis(trifluoromethanesulphonyl9imide. *Electrochim. Acta* **2008**, *53*, 6397–6401. [CrossRef]
35. Appetecchi, G.B.; Montanino, M.; Passerini, S. Ionic liquid-based electrolytes for high-energy, safer lithium batteries. *ACS Symp. Ser.* **2012**, *1117*, 67–128.
36. Lee, W.; Muhammad, S.; Sergey, C.; Lee, H.; Yoon, J.; Kang, Y.; Yoon, W. Advances in the Cathode Materials for Lithium Rechargeable Batteries. *Angew. Chem. Int. Ed.* **2020**, *59*, 2578–2605. [CrossRef] [PubMed]
37. Sun, X. Advances in spinel Li4Ti5O12 anode materials for lithium-ion batteries. *New J. Chem.* **2014**, *39*, 38–63. [CrossRef]
38. Hassoun, J.; Scrosati, B. Review—Advances in Anode and Electrolyte Materials for the Progress of Lithium-Ion and beyond Lithium-Ion Batteries. *J. Electrochem. Soc.* **2015**, *162*, A2582–A2588. [CrossRef]